J. Amer. Soc. Hort. Sci. 149(2):61–74. 2024. https://doi.org/10.21273/JASHS05354-23

# Mode of Action of Calcium in Reducing Macrocracking of Sweet Cherry Fruit

**Andreas Winkler, Pia Bunger, Paula Morales Lang, Christine Schumann, Martin Brüggenwirth, and Moritz Knoche**

*Institute for Horticultural Production Systems, Leibniz-University Hannover, Hannover, Germany*

**Keywords.** cell wall swelling, cracking, cuticle, microcrack, pectin, permeance, *Prunus avium*, splitting, water potential, water uptake

**Abstract. Rain cracking (hereinafter referred to as macrocracking) severely impacts the production of sweet cherry (*Prunus avium*). Calcium (Ca) sprays can reduce macrocracking, but the reported responses to Ca sprays are variable and inconsistent. The objective of this study was to establish the physiological mechanism through which Ca reduces macrocracking in sweet cherry fruit. Six spray applications of 50 mM $CaCl_2$ had no effect on macrocracking (assessed using a standardized immersion assay) despite a 28% increase in the Ca-to-dry mass ratio. Similarly, during another experiment, there was no effect of up to nine Ca sprays on macrocracking, although the Ca-to-dry mass ratio increased as the number of applications increased. In contrast, $CaCl_2$ spray applications during simulated rain (in a fog chamber) significantly reduced the proportion of macrocracked fruit. Additionally, immersion of fruit in $CaCl_2$ decreased macrocracking in a concentration-dependent manner. Monitoring macrocrack extension using image analysis revealed that the rate of macrocrack extension decreased markedly as the $CaCl_2$ concentration increased. This effect was significant at concentrations as low as 1 mM $CaCl_2$. Decreased anthocyanin leakage, decreased epidermal cell wall swelling, and increased fruit skin stiffness and fracture force contributed to the decrease in macrocracking. There was no effect of $CaCl_2$ on the cuticle deposition rate. Our results demonstrated that Ca decreased macrocracking when applied to a wet fruit surface either by spraying on wet fruit or by incubation in solutions containing $CaCl_2$. Under these circumstances, Ca had direct access to the cell wall of an extending macrocrack. The mode of action of Ca in reducing macrocracking is primarily decreasing the rate of crack extension at the tip of a macrocrack.**

Rain cracking (hereinafter referred to as macrocracking) limits sweet cherry (*Prunus avium*) production in all areas of the world where rainfall occurs during the harvest season (Christensen 1996; Knoche and Winkler 2017). Exposure to rain compromises fruit quantity and quality. The quantity is reduced because significant fruit macrocracking excludes this fruit from the primary (fresh) market. The quality is further impaired because of microcracks in the cuticle. This occurs even in fruit that appears visually perfect (Knoche and Winkler 2017). Both macrocracking and microcracking facilitate and accelerate infection by fruit-rot pathogens (Børve et al. 2000). Additionally, transpiration is increased, leading to accelerated loss of firmness and shine and increased shrivel (Knoche and Winkler 2017). Both factors cause significant loss for the producer, marketer, and consumer.

The mechanism of fruit macrocracking in sweet cherry has been largely determined during the past decade (Brüggenwirth and Knoche 2017; Schumann et al. 2019; Winkler et al. 2015, 2016). The so-called Zipper model has replaced the traditional view that excessive fruit turgor is causal (Winkler et al. 2016). Based on the Zipper model, cracking is a multistep process that ultimately causes the skin to "unzip" in a manner analogous to a ladder or a "run" in a knitted fabric. Essential steps of the Zipper process are as follows: (1) cessation of cuticle deposition during early fruit development and the resulting build-up of cuticular strain (Knoche et al. 2004); (2) microcracking resulting from excessive cuticular strain (Peschel and Knoche 2005) and exacerbating effects of surface moisture and/or high air humidity (Knoche and Peschel 2006); (3) localized water uptake through microcracks (Grimm et al. 2019) and, thus, water penetration into the outer flesh tissues where the osmotic potential is most negative (Grimm and Knoche 2015; Grimm et al. 2020); (4) bursting of the cells of the outer flesh and release into the apoplast of malic acid, which causes damage to the adjacent cells, thus rendering them leaky (Winkler et al. 2015); (5) loss of turgor of the skin cells (caused by leakage and cell bursting and plasmolysis) and the resulting swelling of their cell walls (Schumann et al. 2019); and (6) rupture of the stretched skin caused by decreased cell–cell adhesion, which is associated with cell wall swelling (Brüggenwirth and Knoche 2017). This sequence of events—a causal chain—is consistent with all published results to date. It also accounts for the primary mode of fracture of a stretched skin as being "along" the cell walls rather than "across" the cell walls (Brüggenwirth and Knoche 2017). It further explains the occurrence of pectins on the fracture surface of cracks, which is a consequence of the "along the cell wall" fracture mode (Brüggenwirth and Knoche 2017; Schumann et al. 2019).

The options for increasing the consistency of sweet cherry production by decreasing fruit cracking are currently limited. Rain shelters remain the most reliable means of reducing/avoiding fruit cracking (Børve and Meland 1998). Rain shelters are effective because accumulations of surface moisture are largely prevented. Under most conditions, fruit macrocracking can be eliminated or at least markedly reduced by a rain shelter. Even under a rain

Received for publication 23 Oct 2023. Accepted for publication 13 Dec 2023.
Published online 9 Feb 2024.
We thank Germaine Malon, Simon Sitzenstock, Marcel Pastwa, Hana Weiß, and Peter Grimm-Wetzel for technical support and Sandy Lang and Bishnu P. Khanal for helpful comments regarding an earlier version of this manuscript.
This publication was supported by a grant to M.K. from the Deutsche Forschungsgemeinschaft (KN 402/14-1), the Gisela Foundation, and the open access fund of the Leibniz University Hannover.
M.K. is the corresponding author. E-mail: moritz.knoche@obst.uni-hannover.de.

shelter, an extended period of rainfall will occasionally result in a significant incidence of macrocracking. Based on the Zipper model, a rain shelter protects from macrocracking by reducing the formation of microcracks and preventing localized water uptake and, hence, cell bursting and leakage of malic acid into the cell wall space. Rain shelters have become standard in newly established orchards in regions with high incidences of rainfall during the harvest period in nations where their high capital cost is economic.

A second measure for decreasing macrocracking, and one that is frequently mentioned in the scientific literature, is the spray application of calcium (Ca). Numerous studies of the effects on macrocracking of spray applications of Ca salts have been performed [for a recent review, see Winkler and Knoche (2019)]. Unfortunately, the effects reported are variable and inconsistent. In only a few cases, the Ca content of the fruit was determined. Thus, it remains unclear whether sprays increased the Ca content of fruits. This would be a prerequisite for Ca action on fruit cracking because osmotic effects of Ca salts are rather unlikely (Winkler and Knoche 2019). A lack of significant Ca uptake could account for the lack of the effect of Ca on cracking. A lack of Ca penetration would not be surprising because Ca is a poor penetrant of the cuticle (Winkler and Knoche 2021b). The reason for this is because the Ca cation is divalent, carrying two positive charges, whereas the cuticle is a polyelectrolyte (Schönherr and Bukovac 1973). The resulting Donnan exclusion will hinder penetration. Experimental studies of Ca uptake have demonstrated that Ca uptake into sweet cherry fruit and into the fruit of many other crops is low and largely independent of the accompanying anions and the presence/absence of various surfactants (Schlegel and Schönherr 2002; Winkler and Knoche 2021a, 2021b). Despite the numerous studies of spray applications of Ca in sweet cherry [for an extensive compilation, see Winkler and Knoche (2019)], their presumed mode of action in decreasing macrocracking remains unclear.

The objective of this study was to establish the physiological mechanism through which Ca reduces macrocracking in sweet cherry fruit. First, we quantified the effects of $CaCl_2$ on macrocracking after spray applications and immersion assays. Second, we identified the basis of the effects of $CaCl_2$ on selected steps of the Zipper model. We focused on $CaCl_2$ because previous studies revealed that the partner anions have little effect on cuticular Ca uptake (Winkler and Knoche 2021a).

## Materials and Methods

### Plant materials

Sweet cherry fruit (*Prunus avium*) from the cultivars Burlat, Early Korvik, Gill Peck, Kordia, Merchant, Regina, Sam, and Staccato were sampled from greenhouse-grown or field-grown trees grafted on 'Gisela 5' rootstocks (*P. cerasus* × *P. canescens*) at the Horticultural Research Station of the Leibniz University in Ruthe, Germany (lat. 52°14′N, long. 9°49′E), or in a commercial sweet cherry orchard in Ohndorf, Germany (lat. 52°21′N, long. 9°21′E). All fruit from the field were grown under a rain shelter. An exception was fruit from the cultivar Sweetheart and the breeding clone SPC 232, which were sampled from potted trees grafted on Gisela 3 rootstocks and grown under a rain shelter at the Herrenhausen Campus of the Leibniz University in Hannover (lat. 52°27′N, long. 09°84′E). Fruit were cultivated according to current European regulations for integrated fruit production (Cross 2002; Damos et al. 2015). Only fruit free from visual defects were used for the experiments. All fruit were carefully picked by hand in the early morning hours, placed individually in a plastic crate on soft cellular foam, covered with tissue paper, brought to the laboratory, and either processed on the same day or held at 4 °C for no longer than 24 h.

### Establishing the effect of Ca on macrocracking susceptibility

**Spray applications of Ca under a rain shelter—no rain.** Two experiments were conducted to establish the effects of spray applications of $CaCl_2$ on macrocracking susceptibility. During the first experiment, field-grown and rain-sheltered 'Regina' trees were sprayed weekly to runoff with 50 mM $CaCl_2$, starting 24 d after full bloom (DAFB). Preliminary experiments established that this was the maximum $CaCl_2$ concentration beyond which visible signs of phytotoxicity occurred. A total of nine sprays were applied until maturity. Unsprayed trees served as the control. Each treatment consisted of three blocks of three trees each. There was a minimum of one buffer tree between blocks.

During the second experiment, 'Kordia' trees grown under a rain shelter were used to investigate the effects of the frequency of 50 mM $CaCl_2$ or 50 mM Ca formate spray applications. The surfactant Glucopon 215 UP (BASF, Ludwigshafen, Germany) was added at a concentration of 0.2 $g \cdot L^{-1}$. The number of sprays was varied by beginning the weekly spray applications at 7 weeks, 5 weeks, 3 weeks, or 1 week before harvest. The corresponding numbers of sprays were six, four, two, or one. Unsprayed trees served as the control. Each treatment consisted of three blocks of three trees each, with a buffer tree between blocks. Fruit were sampled at full maturity, selected for uniformity based on color and size, and used for a standardized macrocracking test and Ca analysis.

The macrocracking susceptibility was quantified during both experiments (Weichert et al. 2004; Winkler et al. 2015, 2016). Briefly, two groups of 25 fruit each were incubated at ambient temperature (22 °C) in deionized water, removed from water at regular time intervals, and checked for macroscopic cracks by the naked eye. Uncracked fruit were re-incubated and macrocracked fruit were discarded. Water uptake was also determined during a separate experiment using fruit from the same batch. For this experiment, fruit were weighed, incubated individually in deionized water, removed after 45 and 90 min, blotted carefully with tissue paper, re-weighed, and re-incubated. The rate of water uptake was calculated as the slope of a linear regression fitted through a plot of cumulative fruit mass versus time on an individual fruit basis. Fruits that cracked during the experiment were discarded. The minimum number of replications remaining was nine. Sigmoidal regression models were fitted through plots of the percentage of fruit cracking versus time. Based on the regression equations, the time until 50% of the fruit had cracked ($T_{50}$ in h) was calculated. Multiplying the $T_{50}$ by the rate of water uptake yielded the amount of water uptake required for 50% of the fruit to crack ($WU_{50}$ in mg) (Winkler et al. 2015).

To ascertain whether $CaCl_2$ sprays increased the fruit Ca content, the Ca-to-dry mass ratio was quantified during the immature stage (early stage III, 60 DAFB, six sprays, 'Regina' only) and at the mature stage [nine sprays, 'Regina' (81 DAFB), six sprays, 'Kordia' (69 DAFB)] as previously described (Winkler and Knoche 2021a; Winkler et al. 2020a). The pedicels were removed by cutting flush with the receptacle. Fruits were rinsed three times for 10 s in 10 mM citric acid to remove any adhering

Ca residues; then, they were frozen, crushed, de-pitted, lyophilized, and subsequently dried at 103 °C for a minimum of 3 d. The dried tissue was ground (MM 400; Retsch, Haan, Germany). An aliquot of 1 g was re-dried to a constant mass at 103 °C for 3 to 4 d. A sample of 100 mg of the dried powder was ashed in a muffle furnace (L24/11/B180; Nabertherm, Lilienthal, Germany) at 500 °C. Samples not properly ashed were re-wetted with 200 μL of 1 M HCl and re-ashed using the same settings. The ash was taken up with 2 mL of 1 M HCl and 8 mL deionized water and filtered (MN 640 M; Macherey-Nagel, Dueren, Germany). The filtrate was diluted with deionized water such that the final Ca concentration was inside the measuring window of 0 to 4 $mg \cdot L^{-1}$ Samples were analyzed using an atomic absorption spectrometer (AAnalyst 300; Perkin Elmer, Waltham, MA, USA) equipped with a Ca lumina hollow cathode lamp (wavelength, 422.7 nm; slit width, 0.7 nm) using an air–acetylene flame. To eliminate the interference of Ca by phosphorous (P), lanthanum chloride was added to the solution at a concentration of 1% (Fishman and Downs 1966). Each treatment included 20 fruit per biological replicate, three biological replicates, and two or three technical replications.

**Spray applications of Ca in a fog greenhouse.** The effect of spray applications of $CaCl_2$ at 50 mM during simulated rain was investigated in a fog greenhouse using 'Sweetheart' and 'SPC 232' sweet cherry (Winkler et al. 2020b). Deionized water was applied by a high-pressure pump (SS1B1511; S. Ilario d'Enza, Italy; operated at 10 MPa) and injected through nozzles into a closed fog greenhouse. A dense standing fog was established, which settled on the leaves and fruit and formed a continuous water film on all surfaces. The system was operated intermittently for 5 s every 2 min on 2 consecutive days for 8 h per day. $CaCl_2$ solution was applied using a hand sprayer, directly before fogging, during fogging either every hour ('Sweetheart') or during fogging every 2 h ('SPC 232'). The day after fogging ended, all fruit on each tree were harvested. The total number of fruit and that of cracked fruit per tree were recorded, and the percentages of cracked fruit were calculated. Each treatment comprised five trees equivalent to five replicates.

**Immersion applications of Ca in the laboratory.** For the immersion assays, mature 'Burlat' and 'Early Korvik' fruit were sampled in the field. The pedicel was cut to a length of approximately 5 mm, and the pedicel end and pedicel cavity were sealed using silicone rubber (RTV 3140; Dow Corning, Midland, MI, USA). This procedure restricted water uptake to the fruit surface (Beyer et al. 2002). The silicone was allowed to cure overnight in a cooling chamber at 2 °C. Following equilibration to ambient temperature the next morning (22 °C), fruit were incubated in 0, 1, 3, 10, 30, or 100 mM $CaCl_2$. Cracking and water uptake were both determined using two replicates of 25 fruit each, and the $T_{50}$ and $WU_{50}$ were calculated as described.

### Identifying the mechanistic basis of Ca action

**Effect of Ca on cuticular membrane deposition.** To identify any effects of $CaCl_2$ sprays on the rate of cuticular membrane (CM) deposition, cuticles were sourced from 'Regina' fruit (obtained from the spray application experiment described). Fruit were sampled at the immature stage (early stage III, 60 DAFB, six sprays of 50 mM $CaCl_2$) and the mature stage (81 DAFB, following nine sprays of 50 mM $CaCl_2$). Epidermal segments were excised from the fruit cheek in the equatorial region using a biopsy punch (diameter, 8 mm). The epidermal segments comprised the cuticle, epidermis, hypodermis, and some adhering flesh. The epidermal segments were incubated in 50 mM citric acid buffer (at pH 4, adjusted using NaOH) containing pectinase (90 $mL \cdot L^{-1}$; Panzym Super E flüssig; Novozymes A/S, Krogshøjvej, Bagsværd, Denmark) and cellulase (5 $m \cdot L^{-1}$; Cellubrix L; Novozymes A/S) (Fishman and Downs 1966; Winkler et al. 2020a) at 22 °C. To inhibit microbial growth, $NaN_3$ was added at a final concentration of 30 mM. After the CM had separated from the flesh, it was carefully cleaned using a soft camel hair brush and thoroughly rinsed in deionized water. The isolated CMs were transferred onto polytetrafluoroethylene discs for drying, held above dry silica gel for a minimum of 24 h, and then weighed. Subsequently, the CMs were dewaxed using a chloroform:methanol (1:1 volume:volume) mixture. The dewaxed CMs (DCMs) that were obtained were transferred onto polytetrafluoroethylene discs for drying and held above dry silica gel before they were weighed. The CM mass per unit area was calculated by dividing mass by the original area of the 8-mm disc that was excised (50.3 $mm^2$). A gravimetric thickness was calculated by dividing the mass per unit area by the density of the CM (1200 $kg \cdot m^{-3}$) or that of the DCM (1190 $kg \cdot m^{-3}$) (Petracek and Bukovac 1995).

**Microcracks in the cuticle.** The effect of $CaCl_2$ on the formation of microcracks in the cuticle in the stylar region of mature 'Sweetheart' sweet cherry fruit was established. First, fruit were inspected for microcracks after immersion of the stylar scar region in a solution containing the fluorescent tracer acridine orange at a concentration of 0.1% (weight/volume) for 10 min. Thereafter, the fruit were rinsed with deionized water, carefully blotted using tissue paper, and inspected under incident fluorescent light of a binocular microscope (MZ10F with filter GFP plus excitation wavelength of 440–480 nm and emission wavelength of 510 nm; Leica Microsystems, Wetzlar, Germany). Calibrated digital photographs of a rectangular area with a size of 8.8 × 6.6 mm with the stylar scar in the center were obtained. The fluorescing area, the number of microcracks in the microscope window, their mean length, and their cumulative length were quantified using image analysis (cellSens Dimension 1.7.1; Olympus, Hamburg, Germany). This procedure established the extent of microcracking at the beginning of the experiment. Thereafter, microcracks were induced by incubating fruit for 2, 4, 8, and 24 h in 50 mM $CaCl_2$ or in deionized water as a control at 22 °C. At the end of the induction period, fruit were removed from solution, blotted dry, and re-assessed for the extent of microcracking in the stylar scar region as described. Because of the massive amounts of macrocracking, the fruit incubated for 24 h in water could not be assessed. There was no macrocracking of fruit incubated in $CaCl_2$. This procedure allowed calculation of the changes in the fluorescing area, in the number of microcracks per fruit in the stylar region, in the cumulative crack length, and in the length per microcrack on an individual fruit basis. The minimum number of individual fruit replicates was seven. Fruit that cracked macroscopically were discarded.

**Membrane leakage.** The effect of $CaCl_2$ on membrane integrity was indexed by quantifying the anthocyanin efflux from flesh discs excised from mature 'Sweetheart' fruit in the presence and absence of malic acid (Winkler et al. 2015). Anthocyanins are localized in the vacuole, and leakage of anthocyanin into the incubation solution implies a damaged plasma membrane and tonoplast. Flesh discs (diameter, 8 mm; thickness, 2 mm; three discs per replicate; $n = 10$) were excised from the

cheek of a fruit using a biopsy punch and parallel razor blades (2-mm distance between blades). Discs were blotted, rinsed with isotonic sucrose solution, blotted again, and incubated in 0, 1, 3, 10, 50, or 100 mM $CaCl_2$ with or without 70 mM malic acid at 22 °C. All solutions were adjusted to isotonicity using sucrose to prevent bursting of cells caused by water uptake during incubation. After 8 h, discs were removed from solution, and the incubation solution was sampled to determine anthocyanin concentration. Malic acid at 70 mM was added to those solutions that had no malic acid during incubation. This was necessary to correct for any differences in malic acid and, hence, solution pH because the absorption spectrum of anthocyanin depends on pH (Stavenga et al. 2021). The absorption was determined at 520 nm using a spectrophotometer (Specord 210; Analytik Jena, Jena, Germany). Preliminary experiments established that this wavelength corresponded to the absorption maximum of anthocyanin in sweet cherries.

**Macrocrack elongation.** Elongation of macrocracks (macroscopically visible skin cracks) was quantified for 'Burlat', 'Early Korvik', 'Gill Peck', 'Kordia', 'Merchant', and 'Sam' sweet cherry using the procedure of Schumann et al. (2019). Fruit pedicels were cut to a length of 5 mm. To induce initial macrocracking, fruit were incubated in deionized water at 22 °C and checked repeatedly for macrocracks in the stylar scar region. Fruit that had developed macrocracks with a length of approximately 4 mm in the stylar scar region were selected for the experiment. Groups of six fruit were attached individually to a plexiglass plate using a fast-curing silicone rubber (Dowsil SE 9186 Sealant; Dow Corning) such that the stylar scar faced upward. The plate was positioned in a polyethylene box on two custom-built camera stands, each equipped with four digital cameras (WG-20; Ricoh, Tokyo, Japan) so that each camera viewed one polyethylene box containing six fruit. The incubation solution was held at 22 °C using a thermostat (RC6 CS; Lauda Dr. R. Wobser; Lauda-Königshofen; Germany). The cameras were set in time-lapse mode, and images were recorded every 2 h. This setup allowed the monitoring of macrocrack elongation on an individual fruit basis. The macrocrack length was quantified using an image analysis (cellSens Dimension 1.7.1; Olympus). To minimize errors caused by curvature of the fruit surface, measurements were restricted to a circular area of with a diameter of 15 mm around the stylar scar. The initial rate of macrocrack extension was calculated on an individual fruit basis for the time interval up to 2 h of incubation. Using this setup, the macrocrack extension rate response to the Ca concentration was determined for 0, 1, 3, 10, 50, and 100 mM $CaCl_2$ in 'Early Korvik' and 'Sam' sweet cherries. Additionally, the initial crack extension rate was compared in the presence and absence of 50 mM $CaCl_2$ in 'Burlat', 'Early Korvik', 'Gill Peck', 'Kordia', 'Merchant', and 'Sam' fruit. The number of individual fruit replicates was 12.

**Cell wall swelling.** Cell wall swelling in the presence and absence of $CaCl_2$ and malic acid was studied (Schumann and Knoche 2020). The epidermal segments were excised from the cheek, carefully blotted using soft tissue paper, placed on a microscope slide, and subjected to the following experiments: (1) experiment 1, 0, 50, or 100 mM $CaCl_2$; (2) experiment 2: 0, 50, or 100 mM malic acid; and (3) experiment 3: 25 mM $CaCl_2$ plus 25 mM malic acid or 25 mM $CaCl_2$ plus 50 mM malic acid or 50 mM $CaCl_2$ plus 25 mM malic acid. A droplet of one of these solutions was applied to an epidermal segment on the microscope slide. All experiments were conducted at 22 °C. Immediately after droplet application, the epidermal segments were viewed at ×40 (BX60; Olympus). Calibrated images were obtained (DP73; Olympus). The thickness of the anticlinal walls between two living cells was quantified using an image analysis (cellSense Dimensions 1.7.1; Olympus). The epidermal segments were frozen in the incubation solution at −20 °C, followed by 48-h equilibration at 22 °C. The freezing step was necessary to remove turgor. After freezing, the epidermal segments were reinspected as described. The thickness of the anticlinal cells walls between two adjacent dead cells was also quantified. A total of 10 epidermal segments were prepared from 10 fruit per treatment, and two micrographs were taken per epidermal segment. Two cell walls were measured per micrograph, such that the total number of cell walls investigated was 40 per treatment. The increase in swelling of the cell walls (Δthickness) after turgor removal was calculated by subtracting the cell wall thickness immediately after excision from that after the freeze–thaw cycle.

**Mechanical properties of the fruit skin.** A biaxial tensile test mimics the stress–strain relationships of fruit skin samples experienced during growth and during water uptake (Brüggenwirth et al. 2014). The effects of $CaCl_2$ on cell wall swelling and mechanical properties of excised fruit skins of 'Burlat' sweet cherry were investigated. Cell wall swelling was determined as described. The treatment solutions were 0, 1, 3, 10, 30, or 100 mM $CaCl_2$, and all were buffered with 10 mM 2-(N-morpholino)ethanesulfonic acid. The pH was adjusted to 5.8 using KOH. After termination of the 16-h incubation period at 22 °C, the epidermal segments were transferred to a microscope slide on the stage of the microscope (BX60; Olympus). Cell wall swelling was determined before and after a freeze–thaw cycle.

To determine the mechanical properties of the skin, a washer (inner diameter, 12 mm) was glued to one of the two shoulders of a sweet cherry using cyanoacrylate adhesive (Loctite 406; Henkel/Loctite Deutschland, Munich, Germany). After curing, a skin segment was excised by cutting horizontally underneath the washer using a razor blade. Using this procedure, a skin segment was obtained and held in the washer that maintained the in vivo strain of the fruit skin (Knoche and Peschel 2006). The segments were incubated for 16 h at 22 °C in the aforementioned treatment solutions, rinsed with deionized water, and mounted in a custom-made elastometer (Brüggenwirth et al. 2014). The elastometer comprised a custom-made plexiglass chamber that was filled with silicone oil (Wacker AK10; Wacker Chemie, Munich, Germany). The skin segments with the washer were mounted in the lid of the plexiglass chamber. After the removal of air bubbles, a motorized piston was driven into the chamber. The piston displaced the oil, reduced the volume of the chamber, and caused the skin segment to bulge. During this process, the pressure inside the container (pressure sensor type 40PC100G; Honeywell International, Morristown, NY, USA) and the extent of bulging (force transducer KAP-S/5N; AST Angewandte System Technik, Wolnzach, Germany; mounted in a BXC-FR2.5TN material testing machine; Zwick, Ulm, Germany) were monitored. The material testing machine was programmed such that the transducer probe touched the fruit skin with an initial force of 0.05 N. The increases in bulging and pressure inside the chamber were monitored until the skin fractured. The number of replicates was 12. The pressure at fracture and corresponding strain at fracture are referred to as fracture pressure ($p_{fracture}$, kPa) and fracture strain ($\varepsilon_{fracture}$, $mm^2 \cdot mm^{-2}$). The fracture strain was calculated assuming a spherical shape of the bulging skin segment (Brüggenwirth et al. 2014). The modulus of elasticity ($E$) is a measure of the

stiffness of the fruit skin and was calculated according to the following:

$$E = \frac{p*r^2*(r^2 + h^2)}{h^3*t*2}$$

In this equation, $r$ (mm) is the radius of the washer orifice, $p$ (MPa) is the pressure, $h$ (mm) is the height of the bulging skin segment, and $t$ is the thickness of the load-bearing layer ($t$ = 0.1 mm) (Brüggenwirth et al. 2014).

After fracture, the fracture surfaces were inspected using microscopy (BX60; Olympus). The total number of cells along a length of fracture and the number of occasions when these cells separated along their cells walls or across their cell walls were counted. The number of replicates was 12.

**Data analyses.** Data in Figs. 1–5 and 7–9 are presented as means ± *SE*. The only exception is in Fig. 6, where individual replicates are shown. When error bars are not visible in a graph, they are smaller than the plotted symbols. Data were examined by correlation analyses, regression analyses, analyses of variance and Tukey's Studentized *t* test and range test at $P \leq 0.05$ using SigmaPlot (SigmaPlot 12.5; Systat Software, San Jose, CA, USA), R (R version 3.6.3; R Foundation for Statistical Computing, Vienna, Austria), or SAS (version 9.4; SAS Institute, Cary, NC, USA).

## Results

### The effect of Ca on cracking susceptibility

**Spray applications of Ca under a rain shelter: No rain.** Nine $CaCl_2$ sprays at 50 mM had no effect on fruit cracking as compared with the unsprayed control (Fig. 1). In both the treatment and control groups, the percentage of cracked fruit increased in a sigmoidal pattern (Fig. 1). There was no difference in the percentage of cracked fruit between fruit that had been sprayed nine times with $CaCl_2$ and the unsprayed control fruit. This lack of response occurred despite a 28% increase in the Ca-to-dry mass ratio (Table 1).

Increasing the frequency of $CaCl_2$ sprays in the field increased the Ca-to-dry mass ratio up to two applications; further applications had no significant effect (Fig. 2A). There was a slight decrease in the cumulative water uptake or rate of water uptake (Fig. 2B). This decrease was significant for one, four, and six applications. Spray applications of Ca formate had similar effects. There was little effect of the frequency of spray applications on the amount of fruit cracking (Fig. 2C). Essentially all fruit cracked rapidly and completely within 12 h when incubated in deionized water. There was only a small and inconsistent effect of the number of Ca applications on the $T_{50}$ and the $WU_{50}$ (Fig. 2C–F). The $T_{50}$ and $WU_{50}$ increased from zero to two applications; however, with four or six applications, the effect was not significant. There was no difference in the $T_{50}$ with $CaCl_2$ and that with Ca formate (Fig. 2D). The $WU_{50}$ was significantly higher for Ca formate than for $CaCl_2$ (Fig. 2F). The relationship between the $T_{50}$ and Cato-dry mass ratio (r = 0.66*) was weak, and that between the $WU_{50}$ and Ca-to-dry mass ratio (r = 0.26) was not significant (Fig. 3).

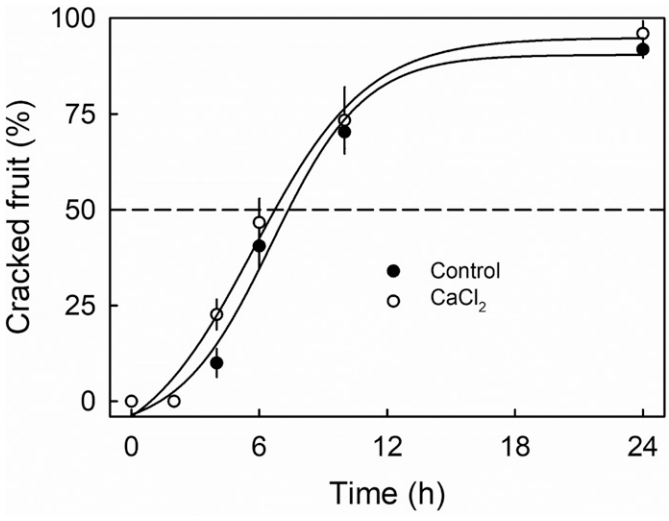


Fig. 1. Time course of cracking of 'Regina' sweet cherry fruit after the application of nine sprays of $CaCl_2$ at 50 mM. Unsprayed fruit served as control. Fruit was harvested at commercial maturity and incubated in deionized water to induce cracking.

Table 1. Effect of weekly applications of 50 mM $CaCl_2$ on the amount of calcium (Ca) per fruit and the Ca-to-dry mass ratio of early stage III and mature stage III 'Regina' sweet cherry fruit. The early stage III sweet cherry fruit received six Ca applications and the mature stage III fruit received nine applications. Unsprayed fruit served as control.

| | Total Ca (mg per fruit) | | Ca/dry mass ratio ($mg \cdot g^{-1}$ DM) | |
|---|---|---|---|---|
| Treatment | Early stage III | Mature stage III | Early stage III | Mature stage III |
| Control | 1.02 ± 0.03 | 1.23 ± 0.06 | 1.16 ± 0.06 | 0.65 ± 0.02 |
| $CaCl_2$ | 1.28 ± 0.07* | 1.45 ± 0.06* | 1.27 ± 0.05 | 0.83 ± 0.03* |

Data are presented as mean ± *SE*.
*Significant difference compared with the control and Studentized *t* test ($P \leq 0.05$).

**Spray applications of Ca in a fog greenhouse.** Spray applications of $CaCl_2$ during simulated rain significantly decreased fruit cracking of both cultivars (Table 2). Fruit from 'SPC 232' was more susceptible to cracking than that from 'Sweetheart'.

**Immersion applications of Ca in the laboratory.** Water uptake increased linearly with time; there was no effect of $CaCl_2$ on the rate of water uptake in 'Kordia' and only a slight decrease in that rate in 'Burlat' (Fig. 4A and B). The percentage of cracked fruit increased with time (Fig. 4C) and with water uptake (Fig. 4E), but at a lower rate with $CaCl_2$ in the incubation solution. Expressing the $T_{50}$ and $WU_{50}$ as functions of the $CaCl_2$ concentration revealed biphasic relationships with breakpoints at approximately 10 mM $CaCl_2$. At concentrations exceeding this threshold, the $T_{50}$ and $WU_{50}$ increased. In 'Kordia', at 10 mM $CaCl_2$ or lower, the $T_{50}$ and $WU_{50}$ were independent of the $CaCl_2$ concentration, whereas in 'Burlat', even 1 mM $CaCl_2$ increased the $T_{50}$ and $WU_{50}$ approximately three-fold (Fig. 4D and F).

### Identifying the mechanistic basis of Ca action

**Effect of Ca on cuticular membrane deposition.** Spray applications of Ca had no effects on the mass per unit area of the CM or DCM. These null effects occurred at the immature stage after six applications of $CaCl_2$ and at the mature stage after nine $CaCl_2$ applications (Table 3). The CM and DCM were both thicker during the immature stage than during the mature stage.

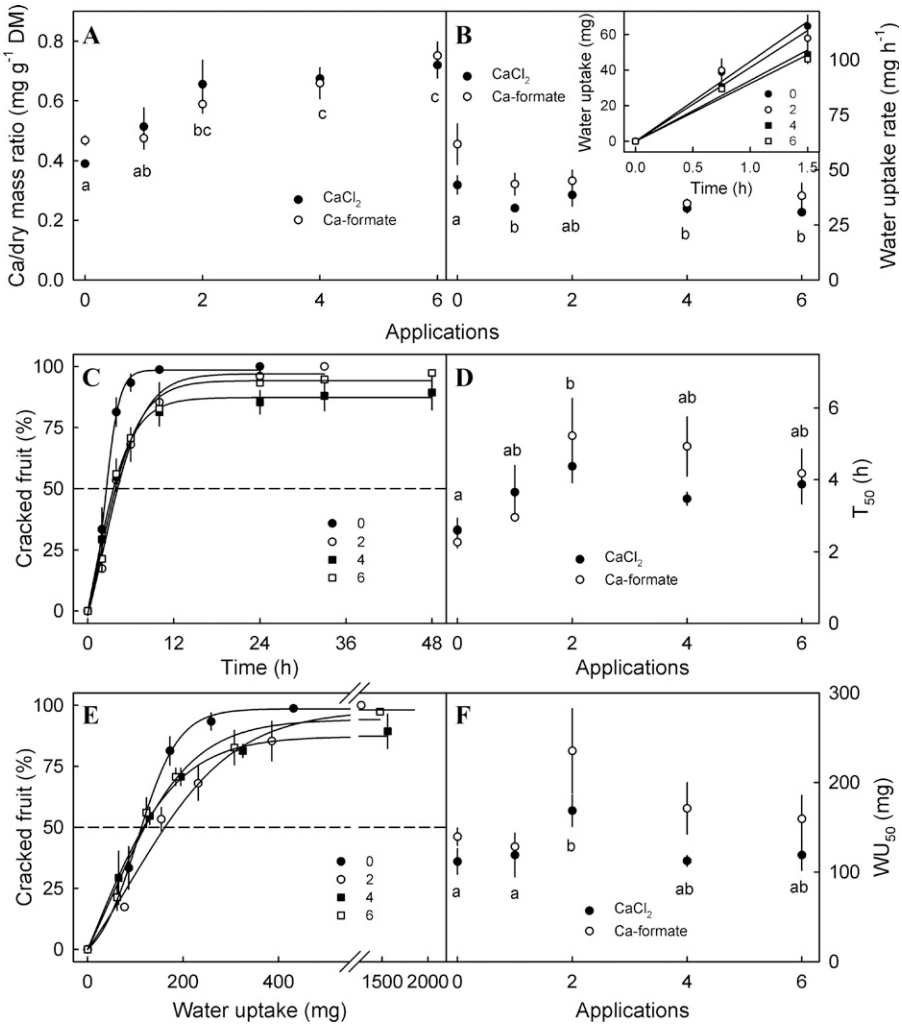


Fig. 2. Effect of the frequency of sprays of $CaCl_2$ and Ca formate on the Ca-to-dry mass ratio, water uptake, Ca uptake, and fruit cracking. Effect of the frequency on the Ca-to-dry mass ratio of 'Kordia' sweet cherry fruit (**A**) on the time course of water uptake (**B**, inset) and rate of water uptake (**B**, main graph). (**C**) Time-course of cracking of fruit that was sprayed up to six times with $CaCl_2$. To induce cracking, the fruit was incubated in deionized water. (**D**) Time to 50% cracking ($T_{50}$) of fruit that was sprayed with $CaCl_2$ and Ca formate up to six times. (**E**) Fruit cracking as affected by the amount of water taken up. (**F**) Amount of water uptake at 50% cracking ($WU_{50}$) of fruit that was sprayed up to six times with $CaCl_2$ and Ca formate. A two-factorial analysis of variance revealed significant main effects for the frequency of application (rate of water uptake, $T_{50}$) and salt (Ca-to-dry mass ratio, rate of water uptake, $T_{50}$, and $WU_{50}$). The interactions of frequency of application and salt were not significant. Means followed by the same lowercase letter do not differ significantly according to Tukey's Studentized range test ($P \leq 0.05$).

**Microcracks in the cuticle.** All fruit used in the experiment showed significant and highly variable microcracking around the stylar scar (as indexed by the area infiltrated with acridine orange) (Fig. 5A–D). Typically, microcracks that occurred were oriented tangentially relative to the stylar scar. Microcracking (as indexed by the area infiltrated with acridine orange) increased as incubation times increased when fruit was incubated in deionized water, but not when incubated in $CaCl_2$. Fruit incubated in water had cracked extensively within 24 h; therefore, microcracking could not be analyzed. In contrast, fruit incubated in $CaCl_2$ remained intact even after 24 h, with no significant increases in the area infiltrated with acridine orange (Fig. 5).

Cumulative crack length, mean length per microcrack, and the number of microcracks were all highly variable, irrespective of incubation time and incubation solution (Fig. 6A, C, and E). However, a regression analysis revealed that the cumulative crack length, mean length per microcrack, and number of microcracks before and after incubation were closely significantly related. Furthermore, calculating the increase in cumulative crack length, mean length per microcrack, and number of microcracks revealed that the increase in the cumulative microcrack length was markedly lower in the presence of $CaCl_2$ as compared with deionized water (Fig. 6B). The effect of $CaCl_2$ resulted primarily from a nearly constant length of microcracks, whereas the length of microcracks markedly increased during incubation in deionized water (Fig. 6D). Apparently, $CaCl_2$ inhibited the extension of microcracks that occurred in water. There was no difference in the increase in the number of microcracks between $CaCl_2$ and water (Fig. 6F).

**Membrane leakage.** Increasing $CaCl_2$ concentrations had a small, albeit significant, effect on anthocyanin leakage in the absence of malic acid. However, when simulating cell bursting by incubating in malic acid, $CaCl_2$ decreased anthocyanin leakage in a concentration-dependent manner. In the absence of $CaCl_2$,

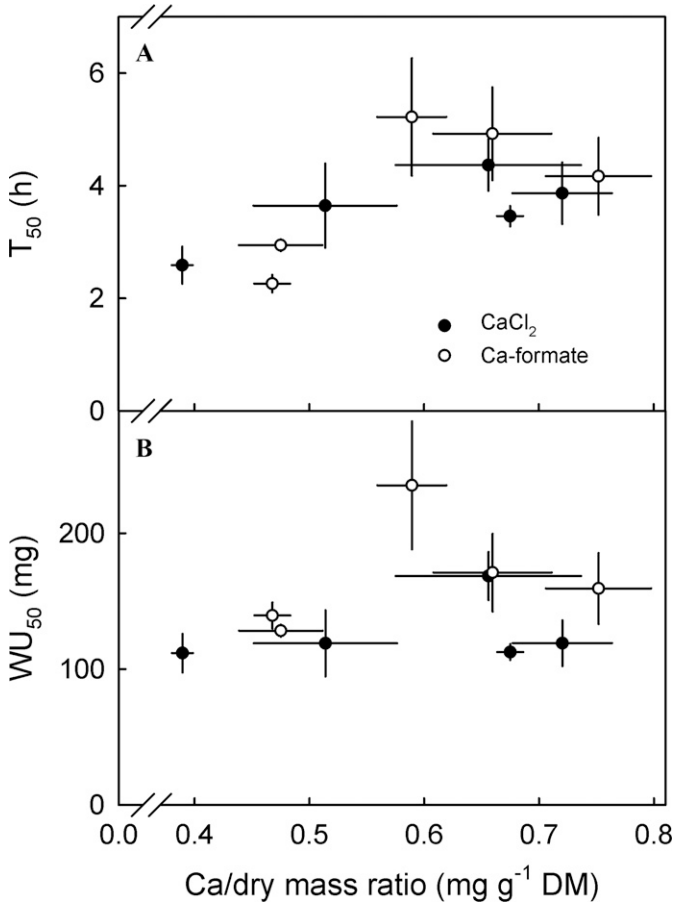


Fig. 3. Relationship between the time to 50% cracking ($T_{50}$) (**A**) or the amount of water needed for 50% cracking ($WU_{50}$) (**B**) and the Ca-to-dry mass ratio of 'Kordia' sweet cherry fruit. The Ca-to-dry mass ratio varied with up to six sprays of $CaCl_2$ or Ca formate.

anthocyanin leakage was markedly increased by malic acid. As the $CaCl_2$ concentration was increased, anthocyanin leakage markedly decreased, indicating that $CaCl_2$ opposed the effect of malic acid (Fig. 7).

**Macrocrack elongation.** When fruit with short macrocracks was incubated in water or $CaCl_2$, crack extension was initially rapid, but then it slowed significantly, as indexed by the decrease in slope. The crack length reached 90% of the maximum length within 12 h (Fig. 8A and B). When incubated in $CaCl_2$, the initial rate of macrocrack extension was inversely related to the $CaCl_2$ concentration. Even low concentrations of $CaCl_2$ (1, 3, and 10 mM) were highly effective in decreasing the initial rate of macrocrack extension. Higher $CaCl_2$ concentrations resulted in little additional effects (Fig. 8C). The response of the initial rate of crack extension to different $CaCl_2$ concentrations did not differ between the two cultivars examined. The decrease in the initial rate of crack extension caused by $CaCl_2$ was consistent and significant in all six cultivars investigated (Table 4).

**Cell wall swelling.** Releasing the turgor by a freeze–thaw cycle resulted in significant cell wall swelling. The increase in swelling was lower in the presence of $CaCl_2$ than in its absence (Table 5). In contrast, malic acid markedly increased cell wall swelling as compared with the water control. Cell walls swelled more with 100 mM malic acid than with 50 mM. Combining $CaCl_2$ and malic acid revealed that $CaCl_2$ partly offsets the increase in swelling caused by malic acid (Table 5).

**Mechanical properties of the fruit skin.** Incubating skin segments in $CaCl_2$ had no effect on cell wall thickness when epidermal cells were turgid. However, $CaCl_2$ at concentrations up to 3 mM markedly decreased cell wall swelling when cells were flaccid after turgor had been eliminated by a freeze–thaw cycle. Higher concentrations of $CaCl_2$ had no additional effect on decreasing cell wall swelling (Fig. 9A). The cell wall's modulus of elasticity increased up to 3 mM $CaCl_2$ and the fracture pressure increased up to 100 mM (Fig. 9B and C). There was no significant effect on the strain at fracture (Fig. 9C, inset). $CaCl_2$ also affected the fracture mode. Increasing the concentrations of $CaCl_2$ decreased the percentage of occasions when cells separated along the cell walls (cell–cell separation along the middle lamella) and increased the percentage of occasions when cells separated across cell walls (cell walls fractured) (Fig. 9D).

Table 2. Effect of spray applications of $CaCl_2$ at 50 mM during simulated rain on the percentage of cracked sweet cherry fruit. Potted trees were exposed to simulated rain for 8 h on two consecutive days and sprayed with 50 mM $CaCl_2$ before the rain began in the morning, every 2 h (SPC 232) and every 1 h (Sweetheart) during the rain, and immediately after the rain was switched off.

| | Cracked fruit (% of total) | | |
|---|---|---|---|
| Treatment | SPC 232 | Sweetheart | $Mean_{cultivar}$ |
| Control | 56.1 ± 5.7 | 20.9 ± 6.9 | 38.5 ± 7.2 a |
| $CaCl_2$ | 38.6 ± 6.0 | 8.2 ± 3.1 | 23.4 ± 6.0 b |
| $Mean_{treatment}$ | 47.4 ± 4.9 a[i] | 14.5 ± 4.1 b | |

[i] A two-factorial analysis of variance revealed significant main effects for cultivar and treatment solution; the interaction was not significant. Mean separation within main effects by Tukey's Studentized range test ($P \leq 0.05$).
Data are presented as mean ± *SE*.

## Discussion

Our study resulted in several important findings:

1. $CaCl_2$ had no effect on cracking when applied as a spray on a dry fruit surface but decreased cracking when sprayed on a wet surface or when applied in an immersion assay.
2. $CaCl_2$ significantly decreased the extension of microcracks and macrocracks. This was probably a result of reduced cell wall swelling, decreased membrane leakage in the presence of malic acid, and improved mechanical properties of the fruit skin. $CaCl_2$ did not increase cuticle deposition.

### Ca reduces cracking on wet, but not on dry, fruit surfaces

Sprays are typically applied during dry periods on dry surfaces, but not during rain on wet surfaces. Our results demonstrated that repeated spray applications of $CaCl_2$ on dry fruit surfaces increased the Ca-to-dry mass ratio of the fruit by up to 83% compared with the unsprayed control. However, $CaCl_2$ sprays had no significant effect on cracking susceptibility, as assessed by an immersion assay (Fig. 1 for 'Regina'; Fig. 2 for

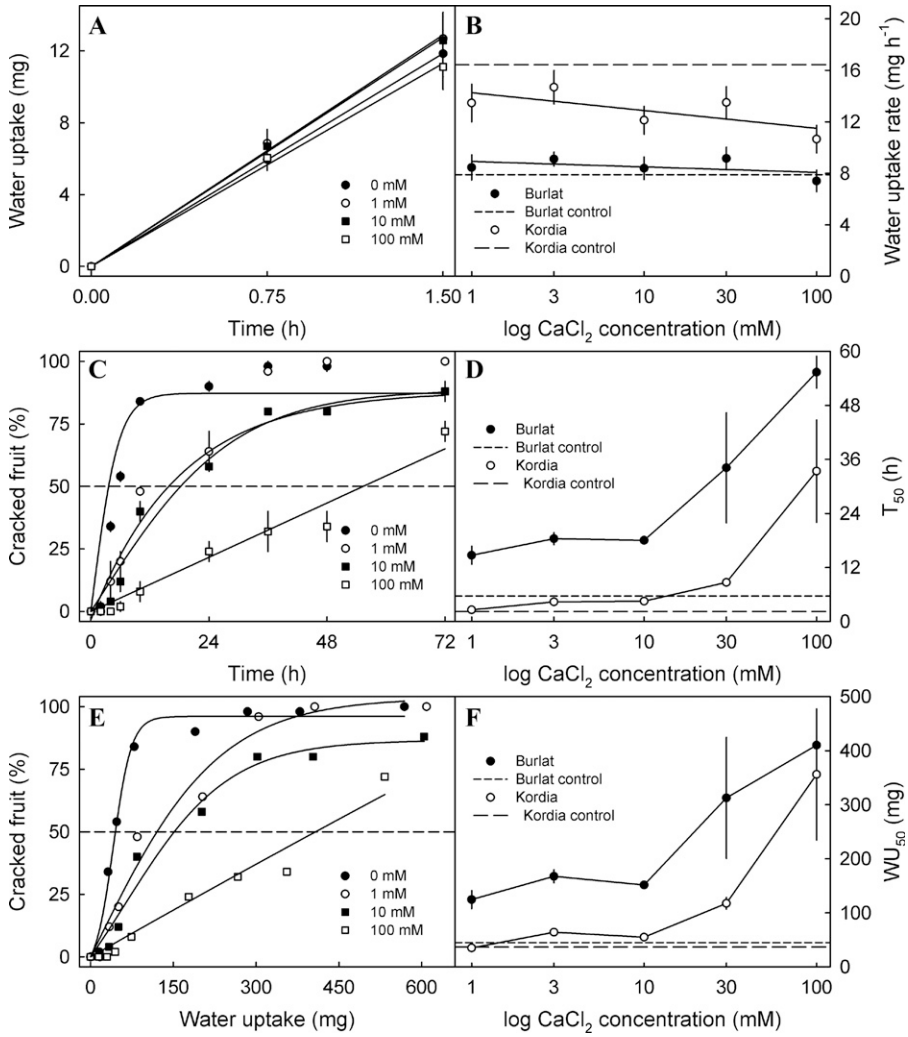


Fig. 4. Effect of the concentration of $CaCl_2$ in the incubation solution on water uptake and cracking of 'Burlat' and 'Kordia' sweet cherry fruit. (**A**) Time course of water uptake. (**B**) Rate of water uptake as a function of the concentration of $CaCl_2$. (**C**) Time course of cracking. (**D**) Time to 50% cracking ($T_{50}$) as a function of the concentration of $CaCl_2$. (**E**) Fruit cracking as a function of the amount of water taken up. (**F**) Water uptake needed for 50% cracking ($WU_{50}$) as a function of the concentration of $CaCl_2$. Dashed horizontal lines in **C** and **E** indicate $T_{50}$ (**C**) and $WU_{50}$ (**E**) of the controls. In **A**, **C**, and **E**, only data from 'Burlat' are shown.

'Kordia'). This observation confirmed the results of the studies that found no effects of in vivo $CaCl_2$ sprays on reducing cracking but did find that cracking was reduced by in vitro incubation in solutions containing Ca ions [see compilation by Winkler and Knoche (2019)]. During two independent experiments, our study found no $CaCl_2$ effect on cracking despite a significant increase in the fruit Ca content and, hence, the Ca-to-dry mass ratio. However, when $CaCl_2$ was applied to fruit in the process of

Table 3. Effect of weekly applications of 50 mM $CaCl_2$ on the mass per unit area of the cuticular membrane (CM) and the dewaxed CM (DCM) of early stage III and mature stage III 'Regina' sweet cherry. The early stage III sweet cherry fruit received six applications and the mature stage III fruit received nine applications. CM and DCM from unsprayed fruit served as control.

| | Mass ($g \cdot m^{-2}$) | | | |
|---|---|---|---|---|
| | CM | | DCM | |
| Treatment | Early stage III | Mature stage III | Early stage III | Mature stage III |
| Control | 1.56 ± 0.02[i] (1.30 ± 0.02)[ii] | 1.34 ± 0.02 (1.12 ± 0.02) | 1.16 ± 0.02 (0.97 ± 0.01) | 1.02 ± 0.02 (0.85 ± 0.02) |
| $CaCl_2$ | 1.49 ± 0.02 (1.24 ± 0.02) | 1.34 ± 0.02 (1.12 ± 0.02) | 1.10 ± 0.02 (0.93 ± 0.01) | 1.00 ± 0.02 (0.84 ± 0.02) |

[i] Data are presented as mean ± *SE*. There are no statistical differences between the $CaCl_2$ and control treatments. Student's *t* test ($P \leq 0.05$).
[ii] Numbers in parentheses represent the gravimetric thicknesses calculated from the mass per unit area and a densities of the CM of 1200 $kg \cdot m^{-3}$ and DCM of 1190 $kg \cdot m^{-3}$ (Petracek and Bukovac 1995).

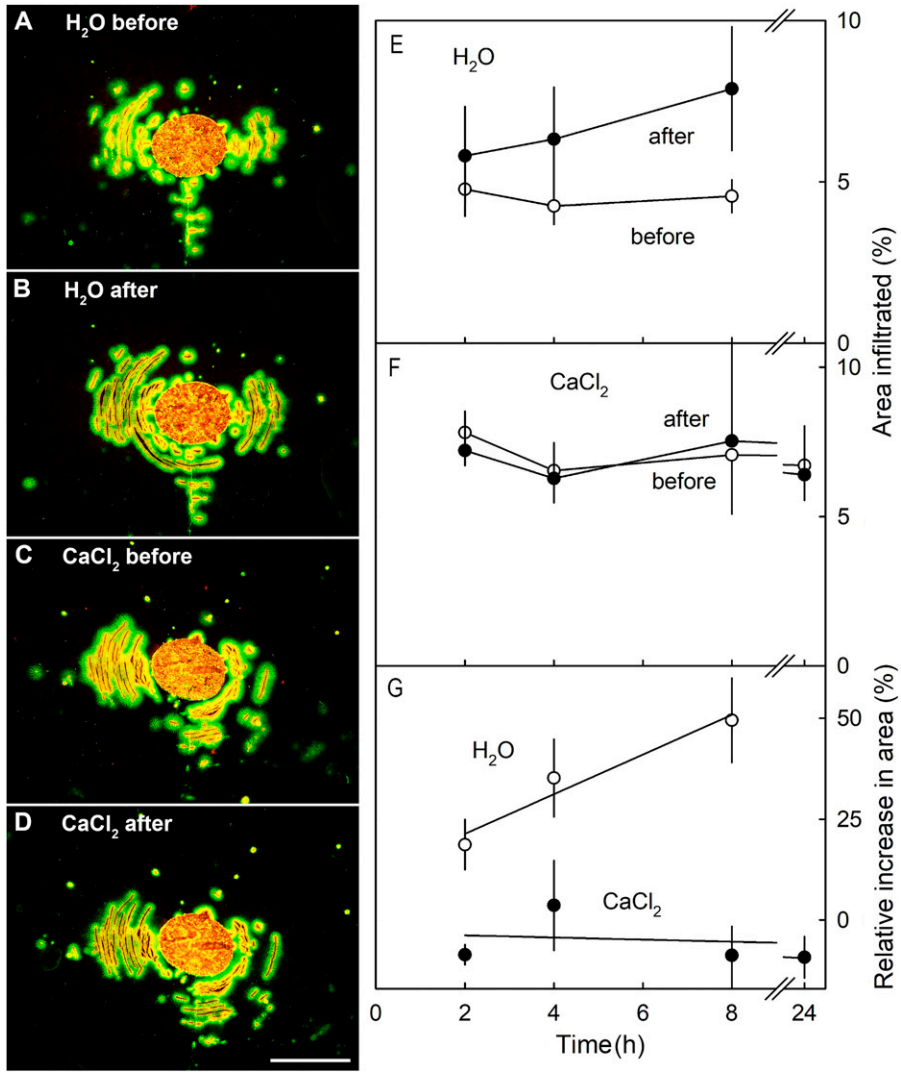


Fig. 5. Effect of submerging mature 'Sweetheart' sweet cherry fruit in deionized water or in 50 mM $CaCl_2$. (**A–D**) Representative fluorescent micrographs of the stylar scar region of sweet cherry fruit before (**A**, **C**) and after 4 h of incubation (**B**, **D**) in deionized water (**A**, **B**) or 50 mM $CaCl_2$ (**C**, **D**). Fruit were incubated for 10 min in the fluorescent dye acridine orange to identify microcracks in the cuticle. Dye penetration is limited to microcracks. An intact cuticle is impermeable to the dye. Scale bar in **D** equals 2 mm. (**E–G**) Formation of microscopic cracks as indexed by the area infiltrated with acridine orange before and after incubation in deionized water (**E**) or $CaCl_2$ (**F**). (**G**) Increase in microcrack formation during the incubation. The relative increase in infiltrated area was calculated by dividing the difference between the areas infiltrated after and before incubation by the area infiltrated before incubation.

cracking (i.e., fruit surface wet)—regardless of whether the $CaCl_2$ was sprayed on during simulated rainfall or applied directly to the fruit using incubation solutions—cracking decreased significantly, even for very low Ca concentrations. The difference between $CaCl_2$ applied to a dry fruit surface and the latter two cases with $CaCl_2$ presented to a wet fruit surface (by spraying on a wet surface or by incubation) is that in the latter, the Ca ions were in direct contact with the cell walls as cracking occurred or cracks extended. Previous studies demonstrated that surface moisture exacerbates microcracking (Knoche and Peschel 2006) and microcracks develop into macrocracks by lateral and radial extension (Schumann et al. 2019). Based on these observations, we inferred that Ca acts directly on the new and extending cracks.

**Mode of action of Ca in reducing cracking of sweet cherry fruit**

In the next section, we describe how we used the Zipper model (Brüggenwirth and Knoche 2017; Schumann et al. 2019) to discuss how Ca ions affect the individual processes that ultimately result in cracking of sweet cherry fruit (Fig. 10).

**No effect of $CaCl_2$ on cuticle deposition**

Our experiments demonstrated that nine sprays of 50 mM $CaCl_2$ between stage II and mature stage III had no effect on cuticle deposition. The lack of an effect on cuticle deposition also excluded potential effects on cuticle strain (Khanal et al. 2014). The absence of an effect of Ca on cuticle deposition was consistent with the following findings. First, cuticle deposition in sweet cherry is limited to stage I and stage II development (Alkio et al. 2012; Grimm et al. 2012; Peschel et al. 2007). Additionally, during a comparison of 31 sweet cherry genotypes, there was no genetic variation in the pattern of cuticle formation (Peschel and Knoche 2012). Second, there was no evidence from any of the recent reviews that Ca plays a role in cuticle formation or affects cuticle deposition (Lara et al. 2014, 2019; Martin and Rose

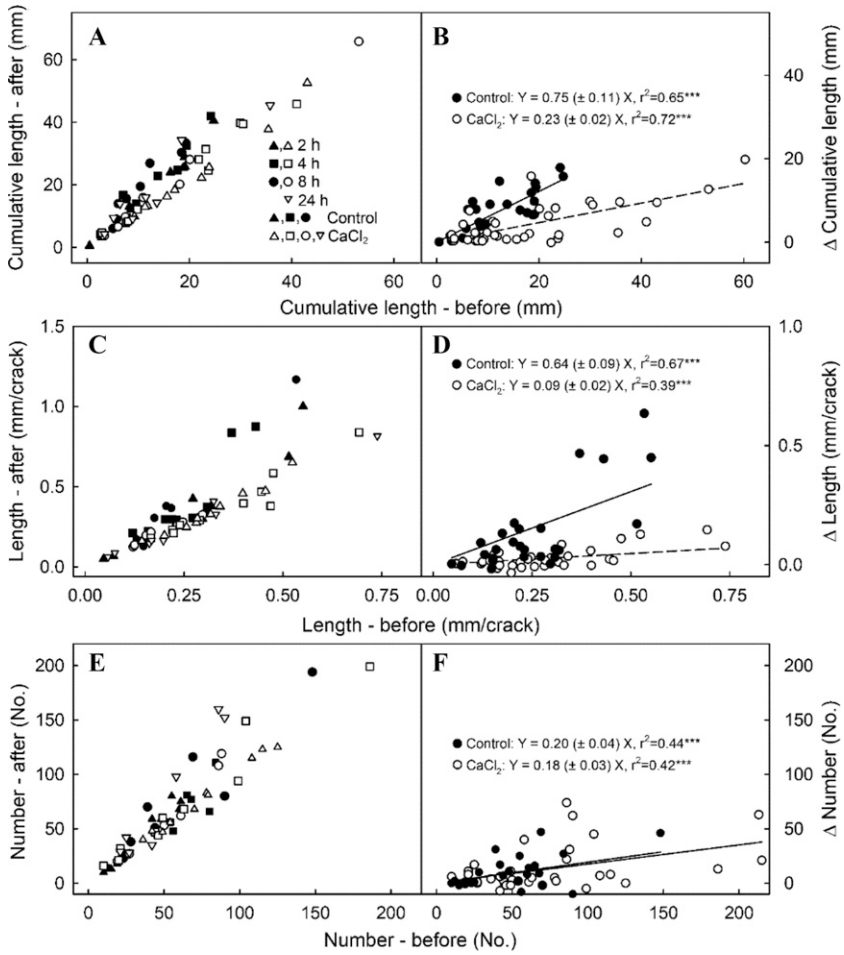


Fig. 6. Effect of submerging mature 'Sweetheart' sweet cherry fruit in deionized water or 50 mM $CaCl_2$ for 2, 4, 8, or 24 h on microcracking of the cuticle. (**A**) Cumulative length of microcracks after incubation, (**B**) the change in the cumulative length of microcracks during incubation, (**C**) the length per microcrack after incubation, (**D**) the change in length per microcrack during incubation, (**E**) the number of microcracks after incubation, and (**F**) the change in the number of microcracks during incubation. Data for the control for 24 h were excluded because all fruit of this treatment severely cracked during incubation. Data points represent individual fruit. Because the y-axis intercept did not differ significantly from zero, regression lines in **B**, **D**, and **F** were forced through the origin.

2014; Yeats and Rose 2013). The only exception occurred during a study by Correia et al. (2020), who reported a 50% increase in cuticle thickness (from 2.5 μm to 3.8 μm) within 4 d of $CaCl_2$ spraying. These findings are difficult to explain and may be artefactual because cuticle deposition would have ceased at the developmental stage of that study because of downregulation of the genes involved in cutin and wax formation and deposition (Alkio et al. 2012). The very rapid change in cuticle thickness was also surprising because $CaCl_2$ penetration is slow (Winkler and Knoche 2021a, 2021b). Finally, the cuticle thickness estimates of Correia et al. (2020) were unusually high in both the sprayed and control fruit. Previous studies reported much thinner cuticles in sweet cherry, which usually fall within the range of 0.71 μm (thin, 'Rainier') to 1.34 μm (thick, 'Kordia') (Peschel and Knoche 2012). Whether Ca salts applied during stage I have an effect on cuticle deposition is currently unknown.

**Ca counteracts the effect of malic acid**

The absence of a marked effect of $CaCl_2$ on anthocyanin leakage in the absence of malic acid revealed that Ca had little or no effect on membrane permeability. Because the solutions were osmotically buffered, cell wall strength was not probed during this experiment.

However, when flesh discs were incubated in malic acid, anthocyanin leakage increased markedly. Increasing the Ca concentration decreased the leakage, indicating that the damaging effects of malic acid were mitigated by Ca. Malic acid is a major osmolyte in sweet cherry juice and released from the vacuole into the apoplast when cells burst (Martin and Rose 2014; Simon 1977). When in the apoplast, malic acid increases the membrane permeability of adjacent cells and—in the absence of osmotic buffering—weakens the cell walls, causing a chain reaction during which the initial cell damage spreads to adjacent cells (Fig. 10) (Winkler et al. 2015). Winkler et al. (2015) attributed the weakening effect of malic acid to the following: (1) the cleavage of neutral sugar side chains of cell wall pectin that weakens the cross-linking between the cellulosic cell wall and pectins (Brummell 2006); (2) pH-dependent activation of polygalacturonases (Chun and Huber 1998); and/or (3) desorption and complexing of cell wall-bound $Ca^{2+}$ (Glenn and Poovaiah 1989). These effects are opposed by Ca, thereby slowing the chain reaction that causes cell bursting to spread (Fig. 10).

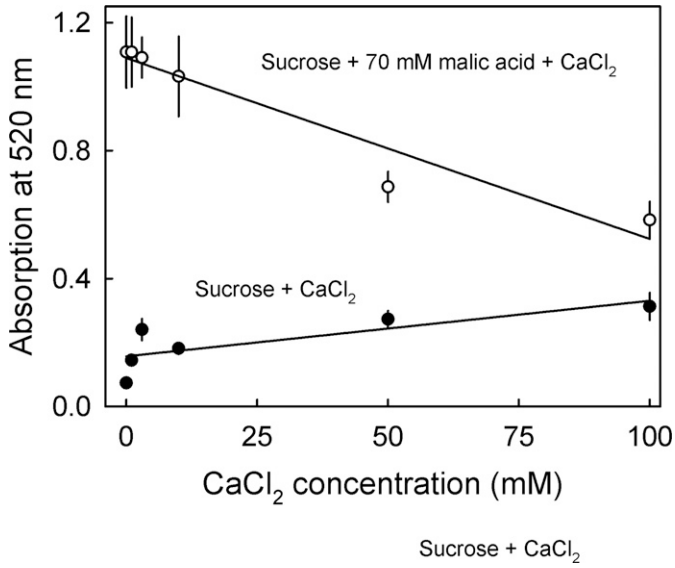


Fig. 7. Effect of the concentration of $CaCl_2$ on anthocyanin leakage from the flesh disc of 'Sweetheart' sweet cherry fruit in the presence and absence of malic acid. All solutions were isotonic to the osmotic potential of the juice of the flesh discs. Regression equations were as follows: sucrose + 70 mM malic acid + $CaCl_2$: absorption = 1.089 – 0.006 × $CaCl_2$ (mM), $r^2$ = 0.36***; sucrose + $CaCl_2$; and absorption = 0.157 + 0.002 × $CaCl_2$ (mM), $r^2$ = 0.32***.

**Ca prevents crack extension**

The Ca ions prevent crack extension when in direct contact with the cell wall. This conclusion is supported by several lines of evidence. First, when fruit with extending macrocracks were submerged in $CaCl_2$, the rate of macrocrack extension was decreased, even at concentrations as low as 1 mM. During this experiment, fruit had first been incubated in water to induce macrocrack development; then, it was selected for the uniform macrocrack length (approximately 4 mm). Thereafter, it was incubated in $CaCl_2$ solution. Similarly, there was no extension of microcracks when fruit surfaces were exposed to solutions containing $CaCl_2$. Both experiments indicated that the Ca ions had direct access to the extending crack without the need for cuticular penetration. Thus, the experiment mimicked Ca spray applications to wet fruit in the field or the incubation of fruit in a solution containing Ca ions during an immersion assay.

Second, Ca gains very rapid entry through a microcrack, thus bypassing the need for the much slower process of penetration through the cuticle. Moreover, a microcrack also serves to focus the incoming Ca on the site of action. In this way, much higher concentrations of Ca will arrive in the exposed cell wall compared with the slow process of cuticular penetration (Winkler and Knoche 2021a). This understanding fits with our observation that microcracking is greatly slowed when a fruit is incubated in $CaCl_2$ and microcracking essentially stops.

Third, previous studies have demonstrated that macrocracking in sweet cherry occurs predominantly by the separation of adjacent cells along the plane of their middle lamellae (Brüggenwirth and Knoche 2017), with the result that pectins are exposed on the surfaces of an emerging macrocrack (Schumann et al. 2019). The dominant component of pectin is galacturonic acid with a $pK_a$ of 3.5 (Kohn and Kovac 1978), which is of the same order of magnitude as the pH of the sweet cherry fruit juice

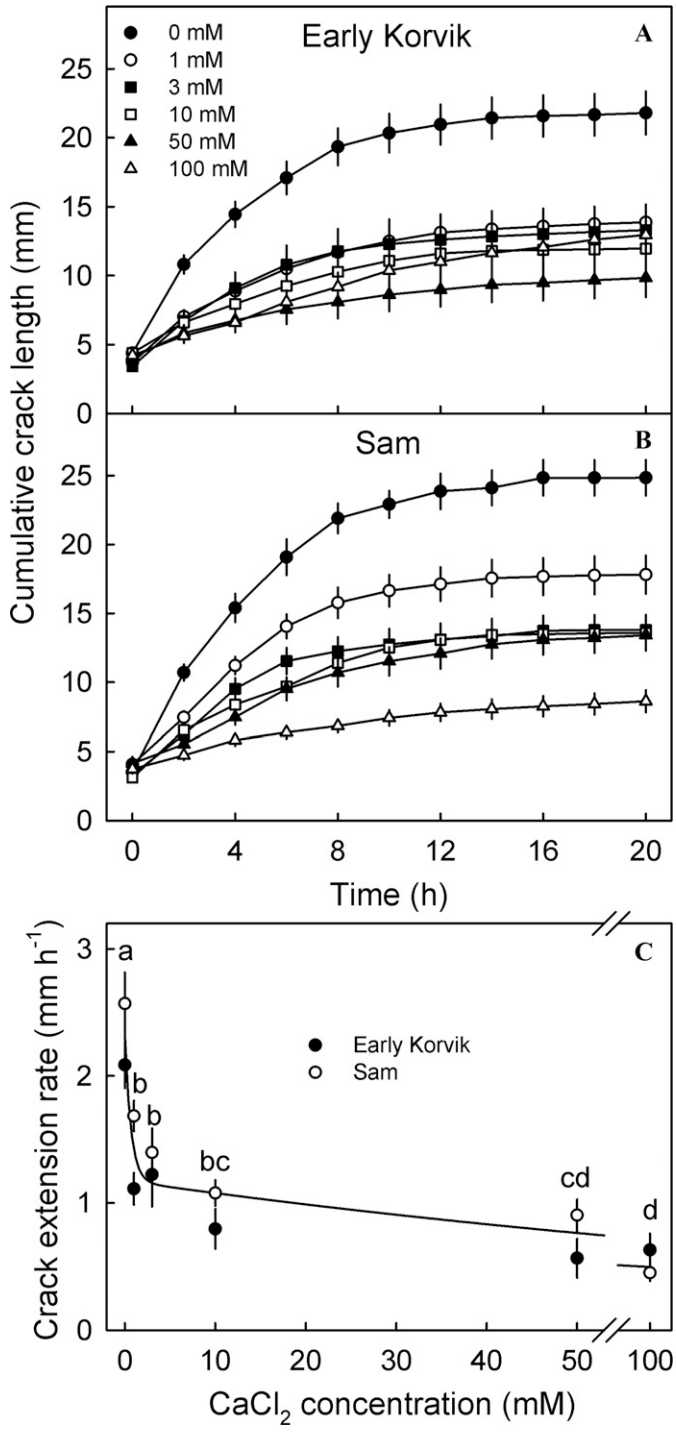


Fig. 8. Effect of the $CaCl_2$ concentration on crack extension in 'Early Korvik' and 'Sam' sweet cherry fruit. (**A**, **B**) Time course of crack extension during incubation of 'Early Korvik' (**A**) or 'Sam' fruit (**B**) in $CaCl_2$ concentrations up to 100 mM. (**C**) Initial rate of crack extension as a function of the $CaCl_2$ concentration. The initial rate of crack extension was calculated with up to 2 h of incubation. A two-factorial analysis of variance revealed a significant main effect for concentration and the two cultivars did not differ. Means followed by the same lowercase letter do not differ significantly according to Tukey's Studentized range test ($P \leq 0.05$).

(Winkler et al. 2015). Upon bursting of cells of the outer mesocarp (Grimm et al. 2019), this juice is leaking into the cell wall space. At this pH, approximately half of the carboxyl groups of the galacturonic acid will carry a negative charge; hence, it will

Table 4. Effect of incubating fruit of different cultivars of sweet cherry in $CaCl_2$ on the initial rate of crack extension. The initial rate of crack extension was calculated for the time interval from 0 to 2 h of incubation. Fruit was precracked to a crack length of approximately 4 mm by incubation in deionized water; thereafter, fruit were incubated in 0 or 50 mM $CaCl_2$. Crack extension was monitored by time-lapse photography and image analysis.

| | Crack extension rate ($mm \cdot h^{-1}$) | | |
|---|---|---|---|
| Cultivar | 0 mM | 50 mM | Ratio |
| Burlat | 2.40 ± 0.31[i] | 0.09 ± 0.03 | 26.9 |
| Early Korvik | 2.37 ± 0.25 | 0.29 ± 0.06 | 8.1 |
| Gill Peck | 3.23 ± 0.32 | 0.73 ± 0.15 | 4.4 |
| Kordia | 2.22 ± 0.26 | 0.25 ± 0.05 | 8.9 |
| Merchant | 3.88 ± 0.31 | 0.68 ± 0.15 | 5.7 |
| Sam | 3.10 ± 0.21 | 0.94 ± 0.14 | 3.3 |
| Grand mean | 2.87 ± 0.26 | 0.50 ± 0.14 | 9.5 |

[i] Data are presented as mean ± *SE*. All pairwise comparisons between 0 and 50 mM $CaCl_2$ treatments are significant according to the Studentized *t* test at $P \leq 0.05$.

serve as an effective sorbent for the Ca cation. Any dilution of the acidic juice in the cell wall space that would occur during rain or incubation would increase the pH and, hence, would increase the charge density, but it would also dilute the Ca dose retained. Under these conditions, Ca would bind to the negative charges, thereby crosslinking the cell wall constituents, particularly in the pectin middle lamellae, resulting in increased cell–cell adhesion.

Fourth, during macrocracking, stresses will concentrate at the crack tip, thereby promoting crack propagation (Brüggenwirth and Knoche 2017; Schumann et al. 2019). Increased cell–cell adhesion at this site is of utmost importance in slowing macrocrack extension, thus effectively jamming the Zipper.

These arguments demonstrate that the beneficial effects of Ca on fruit cracking can be expected if Ca reaches a critical concentration in the cell wall at the tip of a microcrack that then develops into a macrocrack, which then begins to propagate ("run"). This is unlikely the case after applying Ca sprays to a dry fruit surface or following the more general and slower cuticular penetration.

**Effect of Ca on mechanical properties**

The direct incubation of epidermal segments in solutions containing $CaCl_2$ increased the strength of the skin as indexed by increases in both stiffness and fracture force (Fig. 10). In this case, the Ca ions had direct access to the cell walls. The dilution of Ca caused by slow cuticle penetration—as would be the case after spray applications on a dry fruit surface—was not a factor. Thus, the direct access of Ca to the exposed cell walls was identical in a spray application on a wet surface or fruit immersion in a $CaCl_2$ solution.

The effects of $CaCl_2$ on stiffness and fracture force are consistent with those reported previously (Brüggenwirth and Knoche 2017; Schumann et al. 2022). They are accounted for by the crosslinking of cell wall constituents (primarily pectins), as discussed. The increased crosslinking results in increased cell–cell adhesion. The following are indicative of increased adhesion. The first is the decreased cell wall swelling that we observed with Ca in nonturgid, flaccid cells in this and our previous studies (Brüggenwirth and Knoche 2017; Schumann et al. 2022). In intact (turgid) cells, the turgor compresses the cell walls, and this compression is sufficient to prevent cell wall swelling (Schumann and Knoche 2020). The second is a progressive change in fracture mode, from fractures "along" the cell walls to "across" the cell walls (Brüggenwirth and Knoche 2017). The third is the change in micromorphology of cracks reported when sweet cherries were incubated in solutions of the trivalent $FeCl_3$. Cracks in the presence of ferric cations (with three positive charges) were shallow and superficial and did not extend into the underlying epidermal cells, as was the case in the water control (Weichert et al. 2004). Furthermore, cracking was markedly reduced when incubating fruit in solutions of $FeCl_3$ and $CaCl_2$ (Weichert et al. 2004).

In conclusion, multiple applications of $CaCl_2$ (and most likely of other Ca salts, too) may effectively increase the Ca dry mass ratio, but they may not effectively decrease fruit macrocracking. To be effective in reducing macrocracking, the Ca ions must come into direct contact with an extending microcrack that later deepens and develops into a macrocrack and begins to propagate. This response requires direct contact between the cell wall and the Ca solution—for example, in the case of spray application of Ca to a fruit surface that is

Table 5. Effects of $CaCl_2$, malic acid, and combinations of $CaCl_2$ and malic acid on the swelling of cell walls of epidermal cells of mature 'Staccato' sweet cherry. Cell wall thickness was determined before ('+ turgor') and after ('− turgor') a freeze–thaw cycle. The freeze–thaw cycle removed turgor and allowed cell walls to swell. The amount of swelling ('Δ Thickness) was calculated as the thickness of swollen cell walls (without turgor) minus that of nonswollen cell walls (with turgor).

| | | Thickness (μm) | | |
|---|---|---|---|---|
| Expt. | Treatment | + turgor | − turgor | ΔThickness (μm) |
| $CaCl_2$ | Control | 4.3 ± 0.1 a[i] | 7.3 ± 0.2 b | 3.0 ± 0.2 |
| | 50 mM $CaCl_2$ | 4.4 ± 0.1 a | 6.3 ± 0.2 a | 1.9 ± 0.2 |
| | 100 mM $CaCl_2$ | 4.5 ± 0.2 a | 6.4 ± 0.1 a | 1.9 ± 0.2 |
| Malic acid | Control | 4.2 ± 0.1 a | 7.0 ± 0.2 a | 2.8 ± 0.2 |
| | 50 mM malic acid | 4.3 ± 0.1 a | 13.3 ± 0.4 b | 9.0 ± 0.4 |
| | 100 mM malic acid | 4.3 ± 0.2 a | 15.4 ± 0.6 c | 11.1 ± 0.7 |
| $CaCl_2$ + malic acid | 25 mM $CaCl_2$ + 25 mM malic acid | 4.2 ± 0.2 a | 11.5 ± 0.4 b | 7.3 ± 0.5 |
| | 25 mM $CaCl_2$ + 50 mM malic acid | 4.0 ± 0.1 a | 13.6 ± 0.5 a | 9.6 ± 0.5 |
| | 50 mM CaCl2 + 25 mM malic acid | 4.0 ± 0.2 a | 9.2 ± 0.3 c | 5.2 ± 0.3 |

[i] Mean separation within columns and within experiments by Tukey's Studentized range test ($P \leq 0.05$).

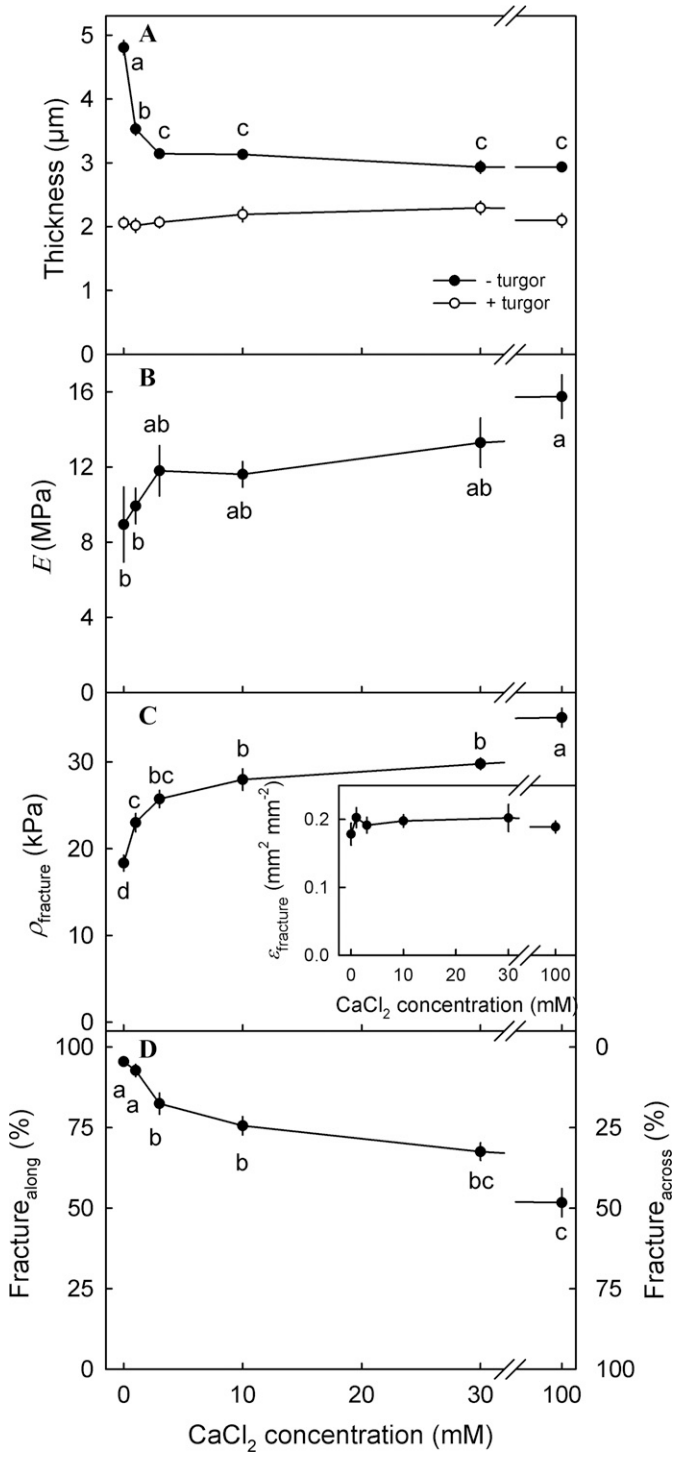


Fig. 9. Effect of $CaCl_2$ at concentrations up to 100 mM on cell wall thickness (**A**) and the mechanical properties in biaxial tensile tests of the skin of mature 'Burlat' sweet cherry fruit (**B**, **C**) or its fracture mode. The mechanical properties were indexed by the modulus of elasticity ($E$) (**B**), the pressure at fracture ($p_{fracture}$) (**C**), and the strain at fracture ($\varepsilon_{fracture}$) (**C**, inset). The fracture mode was quantified as the percentage of cells that fractured along their anticlinal cell walls (**D**). Inset in **D**: Fracture mode as a function of cell wall thickness. Cell wall swelling, mechanical properties, and fracture mode were determined on the same batch of fruit. Cell wall thickness was determined before ('+ turgor') and after ('− turgor') a freeze–thaw cycle. The freeze–thaw cycle removed turgor and allowed cell walls to swell. Data were subjected to an analysis of variance. Data symbols followed by the same lowercase letter were not significantly different according to Tukey's Studentized range test ($P \leq 0.05$). Where no letters are shown, effects were not significant.

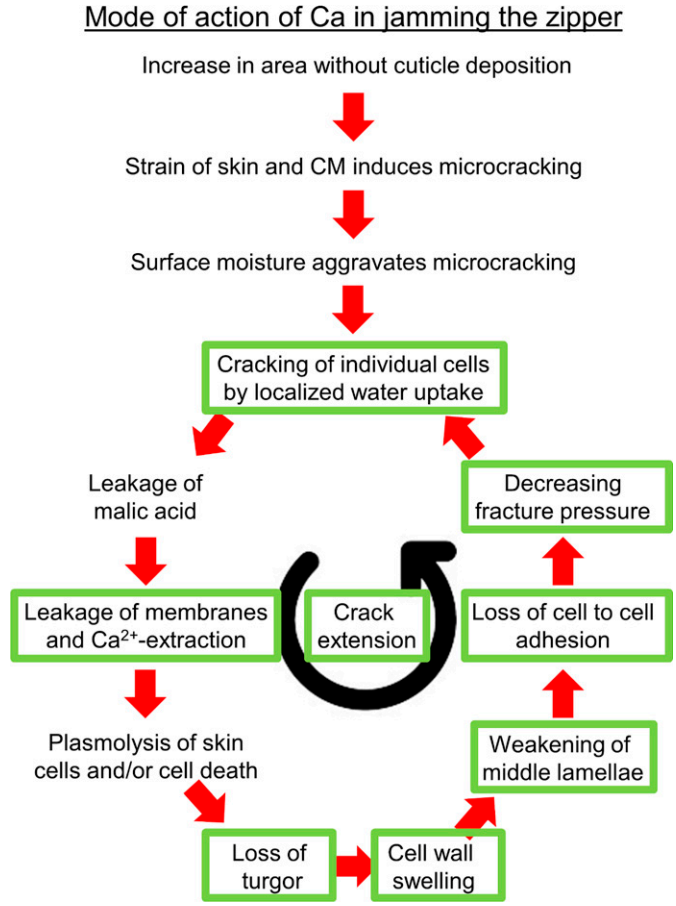


Fig. 10. Sketch illustrating the sequence of events of rain-cracking of sweet cherry fruit as described by the Zipper model and the effects of Ca [Schumann et al. (2019) (modified)]. Processes that are affected by Ca are indicated by the box.

still wet from rain. Only then will Ca ions jam the Zipper by increasing cell–cell adhesion, increasing cell wall stiffness, reducing membrane leakage, and decreasing cell wall swelling.

## References Cited


Alkio M, Jonas U, Sprink T, van Nocker S, Knoche M. 2012. Identification of putative candidate genes involved in cuticle formation in *Prunus avium* (sweet cherry) fruit. Ann Bot. 110(1):101–112. https://doi.org/10.1093/aob/mcs087.

Beyer M, Peschel S, Knoche M, Knörgen M. 2002. Studies on water transport through the sweet cherry fruit surface: IV. Regions of preferential uptake. HortScience. 37(4):637–641. https://doi.org/10.1007/s004250000404.

Børve J, Meland M. 1998. Rain cover protection against cracking of sweet cherries. I. The effects on marketable yield. Acta Hortic. 468:449–453. https://doi.org/10.17660/ActaHortic.1998.468.55.

Børve J, Sekse L, Stensvand A. 2000. Cuticular fractures promote postharvest fruit rot in sweet cherries. Plant Dis. 84(11):1180–1184. https://doi.org/10.1094/Pdis.2000.84.11.1180.

Brüggenwirth M, Fricke H, Knoche M. 2014. Biaxial tensile tests identify epidermis and hypodermis as the main structural elements of sweet cherry skin. AoB Plants. 6:plu019. https://doi.org/10.1093/aobpla/plu019.

Brüggenwirth M, Knoche M. 2017. Cell wall swelling, fracture mode, and the mechanical properties of cherry fruit skins are closely related. Planta. 245(4):765–777. https://doi.org/10.1007/s00425-016-2639-7.

Brummell DA. 2006. Cell wall disassembly in ripening fruit. Funct Plant Biol. 33(2):103–119. https://doi.org/10.1071/Fp05234.
Christensen JV. 1996. Rain-induced cracking of sweet cherries: Its causes and prevention, p 297–327. In: Webster AD, Looney NE (eds). Cherries: crop physiology, production and uses. CAB International, Wallingford, UK. https://doi.org/10.1079/9780851989365.0000.
Chun JP, Huber DJ. 1998. Polygalacturonase-mediated solubilization and depolymerization of pectic polymers in tomato fruit cell walls - regulation by pH and ionic conditions. Plant Physiol. 117(4): 1293–1299. https://doi.org/10.1104/pp.117.4.1293.
Correia S, Santos M, Glinska S, Gapinska M, Matos M, Carnide V, Schouten R, Silva AP, Goncalves B. 2020. Effects of exogenous compound sprays on cherry cracking: Skin properties and gene expression. J Sci Food Agr. 100(7):2911–2921. https://doi.org/10.1002/jsfa.10318.
Cross JV. 2002. Guidelines for integrated production of pome fruits in Europe. Bulletin OILB srop 25:8.
Damos P, Colomar LA, Ioriatti C. 2015. Integrated fruit production and pest management in Europe: The apple case study and how far we are from the original concept? Insects. 6(3):626–657. https://doi.org/10.3390/insects6030626.
Fishman MJ, Downs SC. 1966. Methods for analysis of selected metals in water by atomic absorption. Geological survey water-supply paper 1540-c. U.S. Government Printing Office, Washington, DC, USA. https://doi.org/10.3133/wsp1540c.
Glenn GM, Poovaiah BW. 1989. Cuticular properties and postharvest calcium applications influence cracking of sweet cherries. J Am Soc Hortic Sci. 114(5):781–788. https://doi.org/10.21273/jashs.114.5.781.
Grimm E, Peschel S, Becker T, Knoche M. 2012. Stress and strain in the sweet cherry skin. J Am Soc Hortic Sci. 137(6):383–390. https://doi.org/10.21273/JASHS.137.6.383.
Grimm E, Knoche M. 2015. Sweet cherry skin has a less negative osmotic potential than the flesh. J Am Soc Hortic Sci. 140(5):472–479. https://doi.org/10.21273/JASHS.140.5.472.
Grimm E, Hahn J, Pflugfelder D, Schmidt MJ, van Dusschoten D, Knoche M. 2019. Localized bursting of mesocarp cells triggers catastrophic fruit cracking. Hortic Res. 6. https://doi.org/10.1038/s41438-019-0161-3.
Grimm E, Pflugfelder D, Hahn J, Schmidt MJ, Dieckmann H, Knoche M. 2020. Spatial heterogeneity of flesh-cell osmotic potential in sweet cherry affects partitioning of absorbed water. Hortic Res. 7:51. https://doi.org/10.1038/s41438-020-0274-8.
Khanal BP, Knoche M, Bußler S, Schlüter O. 2014. Evidence for a radial strain gradient in apple fruit cuticles. Planta. 240(4):891–897. https://doi.org/10.1007/s00425-014-2132-0.
Knoche M, Beyer M, Peschel S, Oparlakov B, Bukovac MJ. 2004. Changes in strain and deposition of cuticle in developing sweet cherry fruit. Physiol Plant. 120(4):667–677. https://doi.org/10.1111/j.0031-9317.2004.0285.x.
Knoche M, Peschel S. 2006. Water on the surface aggravates microscopic cracking of the sweet cherry fruit cuticle. J Am Soc Hortic Sci. 131(2):192–200. https://doi.org/10.21273/JASHS.131.2.192.
Knoche M, Winkler A. 2017. Rain-induced cracking of sweet cherries, p 140–165. In: Quero-García J, Iezzoni A, Puławska J, Lang G (eds). Cherries: botany, production and uses. CAB International, Wallingford, UK. https://doi.org/10.1079/9781780648378.0000.
Kohn R, Kovac P. 1978. Dissociation constants of d-galacturonic and d-glucuronic acid and their o-methyl derivatives. Chem Zvesti. 32(4):478–485.
Lara I, Belge B, Goulao LF. 2014. The fruit cuticle as a modulator of postharvest quality. Postharvest Biol Technol. 87:103–112. https://doi.org/10.1016/j.postharvbio.2013.08.012.
Lara I, Heredia A, Dominguez E. 2019. Shelf life potential and the fruit cuticle: The unexpected player. Front Plant Sci. 10:770. https://doi.org/10.3389/fpls.2019.00770.
Martin LB, Rose JK. 2014. There's more than one way to skin a fruit: Formation and functions of fruit cuticles. J Expt Bot. 65(16): 4639–4651. https://doi.org/10.1093/jxb/eru301.
Peschel S, Knoche M. 2005. Characterization of microcracks in the cuticle of developing sweet cherry fruit. J Am Soc Hortic Sci. 130(4):487–495. https://doi.org/10.21273/JASHS.130.4.487.
Peschel S, Franke R, Schreiber L, Knoche M. 2007. Composition of the cuticle of developing sweet cherry fruit. Phytochemistry. 68(7): 1017–1025. https://doi.org/10.1016/j.phytochem.2007.01.008.
Peschel S, Knoche M. 2012. Studies on water transport through the sweet cherry fruit surface: XII. Variation in cuticle properties among cultivars. J Am Soc Hortic Sci. 137(6):367–375. https://doi.org/10.21273/JASHS.137.6.367.
Petracek PD, Bukovac MJ. 1995. Rheological properties of enzymatically isolated tomato fruit cuticle. Plant Physiol. 109:675–679. https://doi.org/10.1104/pp.109.2.675.
Schlegel TK, Schönherr J. 2002. Stage of development affects penetration of calcium chloride into apple fruits. J Plant Nutr Soil Sci. 165:738–745. https://doi.org/10.1002/jpln.200290012.
Schönherr J, Bukovac MJ. 1973. Ion exchange properties of isolated tomato fruit cuticular membrane: Exchange capacity, nature of fixed charges and cation selectivity. Planta. 109(1):73–93. https://doi.org/10.1007/BF00385454.
Schumann C, Winkler A, Brüggenwirth M, Köpcke K, Knoche M. 2019. Crack initiation and propagation in sweet cherry skin: A simple chain reaction causes the crack to 'run'. PLoS One. 14(7): e0219794. https://doi.org/10.1371/journal.pone.0219794.
Schumann C, Knoche M. 2020. Swelling of cell walls in mature sweet cherry fruit: Factors and mechanisms. Planta. 251(3):65. https://doi.org/10.1007/s00425-020-03352-y.
Schumann C, Winkler A, Knoche M. 2022. Calcium decreases cell wall swelling in sweet cherry fruit. Sci Rep. 12(1):16496. https://doi.org/10.1038/s41598-022-20266-9.
Simon EW. 1977. Leakage from fruit cells in water. J Expt Bot. 23(106):1147–1152. https://doi.org/10.1093/jxb/28.5.1147.
Stavenga DG, Leertouwer HL, Dudek B, van der Kooi CJ. 2021. Coloration of flowers by flavonoids and consequences of pH dependent absorption. Front Plant Sci. 11:600124. https://doi.org/10.3389/fpls.2020.600124.
Weichert H, von Jagemann C, Peschel S, Knoche M, Neumann D, Erfurth W. 2004. Studies on water transport through the sweet cherry fruit surface: VIII. Effect of selected cations on water uptake and fruit cracking. J Am Soc Hortic Sci. 129(6):781–788. https://doi.org/10.21273/JASHS.129.6.0781.
Winkler A, Ossenbrink M, Knoche M. 2015. Malic acid promotes cracking of sweet cherry fruit. J Am Soc Hortic Sci. 140(3):280–287. https://doi.org/10.21273/JASHS.140.3.280.
Winkler A, Peschel S, Kohrs K, Knoche M. 2016. Rain cracking in sweet cherries is not due to excess water uptake but to localized skin phenomena. J Am Soc Hortic Sci. 141(6):653–660. https://doi.org/10.21273/jashs03937-16.
Winkler A, Knoche M. 2019. Calcium and the physiology of sweet cherries: A review. Scientia Hortic. 245:107–115. https://doi.org/10.1016/j.scienta.2018.10.012.
Winkler A, Blumenberg I, Schürmann L, Knoche M. 2020b. Rain cracking in sweet cherries is caused by surface wetness, not by water uptake. Scientia Hortic. 269:109400. https://doi.org/10.1016/j.scienta.2020.109400.
Winkler A, Fiedler B, Knoche M. 2020a. Calcium physiology of sweet cherry fruits. Trees. 34:1157–1167. https://doi.org/10.1007/s00468-020-01986-9.
Winkler A, Knoche M. 2021a. Calcium uptake through skins of sweet cherry fruit: Effects of different calcium salts and surfactants. Scientia Hortic. 276:109761. https://doi.org/10.1016/j.scienta.2020.109761.
Winkler A, Knoche M. 2021b. Penetration of sweet cherry skin by $^{45}$Ca-salts: Pathways and factors. Sci Rep. 11(1):11142. https://doi.org/10.1038/s41598-021-90727-0.
Yeats TH, Rose JK. 2013. The formation and function of plant cuticles. Plant Physiol. 163(1):5–20. https://doi.org/10.1104/pp.113.222737.